EARTHQUAKE DEPTH PREDICTIONS USING INFRASONIC WAVES

Douglas O. ReVelle

Los Alamos National Laboratory

Sponsored by National Nuclear Security Administration
Office of Nonproliferation Research and Development
Office of Defense Nuclear Nonproliferation

Contract No. W-7405-ENG-36

ABSTRACT

Having recently examined a U.S. Geological Survey (USGS) data set of ~190 earthquakes and of ~60 mining blasts in the Western USA that occurred during 2000–2002 with corresponding local seismic magnitudes from 3–4.5 over horizontal ranges from 200–1,500 km, we have detected ~20 well defined earthquake signals at the DLIAR large-baseline infrasonic array in Los Alamos. Most of these signals were thermospherically ducted waves. Of the 20 infrasonic earthquake detections, 15 recordings were thermospheric, 11 recordings were stratospheric and 6 recordings were of both types. For infrasonic signals with only a single recorded return, 9 recordings were thermospheric and 5 recordings were stratospheric. One approach, of the numerous types of analyses performed on these waves, assumed that the earthquake signals have identical atmospheric propagation characteristics to those of near-surface atmospheric explosions, with the only exception being that the earthquake source occurred at generally shallow depths (<15 km) within the earth's crust. All of the original calibrated earthquake depths are known parameters from the individual USGS seismic wave solutions (in addition, to source origin time, latitude, longitude, etc.). From this type of analysis, we have produced a strongly correlated relationship connecting the calibrated earthquake depth and the deduced vertical depth scale factor from our infrasonic wave amplitude solutions. This vertical depth scale factor is the required vertical scaling parameter for each earthquake that is needed in order to predict the specific infrasonic wave amplitudes that are identical to those for ducted atmospheric blast waves from a near-surface point source as a function of range and source yield (or equivalently for the concomitant local seismic magnitude). This deduced vertical depth scaling factor was determined using a least-squares curve-fit of observed earthquake depths versus the vertical depth scaling factor for the simple case of a four-parameter Gaussian function. This fitting resulted in a maximum value of $r^2 = 0.831$ by utilizing the observed earthquake depths and the four-channel averages of the peak-to-peak, maximum infrasonic wave amplitudes. Our curve-fitted results can now be used to more realistically forecast earthquake depths as a function of the observed horizontal range (~207–1,370 km), as a function of the observed source yield (or for the local seismic magnitudes from ~3 to 5.5) and finally as a function of the observed infrasonic wave amplitudes (from ~0.007 to 0.12 Pa). It can also be used as a depth discriminant to reliably diagnose earthquake infrasonic signals from mining blast explosion infrasound for sources whose signals are well observed infrasonically and for which ancillary source yields are also available in the absence of simultaneously recorded seismic waveform data.

OBJECTIVES

The objective of this work was to systematically and reliably evaluate the depth of earthquakes on the basis of the detection of their infrasonic signals radiated as a function of horizontal range, source yield (or equivalently the local seismic magnitude) and of the infrasonic wave signal amplitude. Using depth as a key identified parameter, we can then pursue the successful discrimination of earthquakes from near-surface mining blasts using infrasonic waves.

RESEARCH ACCOMPLISHED

We have evaluated the infrasonic signals from ~20 earthquakes (whose seismic magnitude ranged from about 3–5.5) in order to systematically deduce earthquake depth (ReVelle, 2005). This was accomplished using the following key assumption for earthquake zones that also possess the requisite source fault mechanism:

> The propagation of infrasonic signals from earthquakes is otherwise ***identical*** to that of near-surface free air bursts in the atmosphere. The only fundamental difference between these assumed point sources is that "small" earthquakes generally originate at ***shallow*** depths within the earth (<15 km below the surface), which always degrades the recorded signal amplitude. Thus, if we can successfully evaluate a depth correction factor for each earthquake (as a function of range, yield, and infrasonic signal wave amplitude), we can also deduce an empirical relationship between earthquake depth and the vertical depth scale factor due to the source region location beneath the earth's surface.
>
> A curve-fitted analysis of this behavior will allow the general prediction of earthquake depths over a range of observing conditions. The analysis of this predicted, but admittedly overly simplified behavior, is outlined below.

Earthquake Amplitude Coupling to the Atmosphere

We have examined propagating atmospheric blast waves from near-surface "point" sources and have compared the observed earthquake amplitudes as a function of range and source energy (or equivalently in terms of local seismic magnitude), etc. The far-field, quasi-linear, semi-empirical wave propagation amplitude regression equation for free-air, near-ground-level explosions (just above ground level, but not buried) propagating in a thermospheric waveguide in the atmosphere is given by ANSI (1983):

$$\Delta p = K \cdot \{W^c/R\}^B \qquad (1)$$

where

- Δp = peak to peak wave amplitude in μbars
- K = $4.95 \cdot 10^4$ = constant for amplitudes in μbars (1 μbar = 0.10 Pa)
- W = explosive charge weight in kt: TNT equivalent
- c = ½ for far-field conditions ($R >> \lambda$, λ the wavelength at $x = 10$, i.e., $R = 10.0 \cdot R_{ps}$ with $x = R/R_{ps}$)
- R = total horizontal range from source to observation point
- B = 1.36
- $c \cdot B$ = 0.68

The original expression for a stratospheric waveguide also contained the multiplying factor 10^{-kV} on the right hand side of Equation (1), which accounted for stratospheric wind speed propagation effects whose speed regularly exhibited a seasonal direction reversal, with generally small seasonal wind speed changes (where k is a propagation constant). We have implicitly assumed in this analysis that for sufficiently large sources (such that absorption losses are sufficiently small over relatively long propagation paths) that the thermospheric waveguide amplitudes could be modeled using the Stratospheric waveguide results with the wind enhancement/decay factor having been removed.

For an atmospheric point source explosion, the blast wave relaxation radius, R_{ps} is given by Sakurai (1965):

$$R_{ps} \equiv \{E_s/p(z)\}^{1/3} \quad (2)$$

where

p(z) =the ambient atmospheric pressure at the source altitude

Es = the source energy in Joules (where 1 kt of TNT equivalent energy release = $4.185 \cdot 10^{12}$ Joules)

The corresponding wave frequency and wavelength, λ, at maximum amplitude in the atmosphere at x = 10 ($x \equiv 10\ R/R_{ps}$) are given by

$$f = c_s/\{2.21 \cdot R_{ps}\} \quad (3a)$$

$$\lambda = 2.21 \cdot R_{ps} \quad (3b)$$

More recent analyses of weakly nonlinear propagation effects (see Mutschlecner and Whitaker, 2005, for example) have suggested B = 1.45 whereas earlier analyses by Reed (1972a; 1972b) had suggested B = 1.20, so that the value we have used brackets the available measurement possibilities. Since B > 1, this means that some small accumulative weakly nonlinear propagation effects will affect the propagation of the dispersed explosion pulse through the atmosphere. At very large ranges, for sufficiently small amplitude waves compared to the background pressure (where $\Delta p/p << 1$), Δp is proportional to 1/R so that the energy "lost" from the wave has a corresponding geometrical spreading loss that exhibits an inverse square law dependence.

Next, we will also compare earthquake infrasonic propagation through a thermospheric waveguide against the results using Equation (1) by first defining an exponential decaying vertical depth coupling factor, k_{EQ} (because earthquakes deliver their energy to the atmosphere through ground "shaking" after propagation upward from the source below, from various depths below ground level, i.e., below z = 0, after a corresponding propagation time delay, Δt, from the earthquake at depth z to the surface).

$$\Delta p = K \cdot \{W^c/R\}^B \cdot \exp[-k_{EQ} \cdot z] = K \cdot \{W^c/R\}^B \cdot \exp[-z/D_{EQ}] = K' \cdot \{W^c/R\}^B \quad (4)$$

where

z = depth of the earthquake below the ground (z = 0)

k_{EQ} = D_{EQ} where D_{EQ} is the vertical depth scale factor (expressed in km) with k_{EQ} the vertical depth coupling factor (or the vertical depth coefficient), expressed in km^{-1}

K' = amplitude scaling reduction due to the earthquake depth

In essence, multiplying Equation (1) by the exponential factor is another way of saying that the purely atmospheric propagation constant K has now changed to the form $K' = K \cdot \exp[-z/D_{EQ}]$. In this way, assuming all other propagation and fault type factors, etc., are unchanged, we have prescribed a way of determining the vertical depth scale factor, D_{EQ}, assuming that all of the amplitude changes relative to an air-blast situation are due solely to the depth of the earthquake below the surface of the earth. This is obviously an extreme simplification of the complex earthquake source, but one that certainly deserves examination.

Values of k_{EQ} were extracted from the 15 infrasonically detected wave amplitudes (four-channel averaged values) for thermospheric returns using the following expression (except for the indeterminate value in the limit as $z \rightarrow 0$):

$$k_{EQ} = -\ln\{(\Delta p/K)\cdot(W^c/R)^{-B}\}/z = 1/D_{EQ} \quad (5)$$

or after inverting and explicitly solving for the earthquake depth:

$$z = \text{earthquake depth} = -D_{EQ}\cdot \ln\{(\Delta p/K)\cdot(W^c/R)^{-B}\} \quad (6)$$

Plotting the deduced vertical depth scaling factor, D_{EQ}, versus the various earthquake depths available from the seismic data analyses that were deduced automatically by the USGS (recorded over a wide range of horizontal distances, wave amplitudes, and seismic magnitudes), we have been able to determine a well-correlated regression between the earthquake depth and the vertical depth scaling factor:

$$z = y_o + a\cdot\exp[-(1/2)\cdot((D_{EQ} - x_o)/b)^2] \quad (7)$$

or

$$D_{EQ} = x_o \pm b\cdot\{-2\cdot\ln((z-y_o)/a)\}^{1/2} \quad (8)$$

where

$a =$ 24.4795 km ± 30.3779 km

$b =$ 2.1453 km ± 1.7200 km

$x_o =$ 2.1224 km ± 0.1350 km

$y_o =$ -14.9268 ± 30.8003

Of the two solutions available for the square root expression in Equation (8), the negative root is applicable for earthquake source depths < a (in km) for values of the depth scale factor ≤ x_o. For source depths < a with a depth scale factor > x_0, the positive square root of the multi-valued system is applicable.

The Scaled-Energy-Range Concept

We have chosen to plot our results derived above versus either the local seismic magnitude or versus the scaled energy-range. The seismic magnitude and its conversion to energy will be discussed next. The general relationship that was used in order to convert between the Richter (local) seismic magnitude, M_R, and the source energy expressed in kt (TNT equivalent) is as follows:

$$\log(W(\text{kt TNT equivalent})) = \{1.50\cdot M_R - 6.0\} \quad (9a)$$

or

$$M_R = (2/3)\cdot\{\log(W(\text{kt TNT equivalent})) + 6.0\} \quad (9b)$$

The dimensionless scaled-energy range concept is simply a way of simultaneously combining the two separate parameters of source energy (or equivalently, the charge weight expressed in kt, for example) and range and is contained within the amplitude relationship, Equation (1), after normalization for thermospheric returns. The scaled energy-range can be written using Equation (1) after first dividing through by K, the leading constant propagation factor:

$$\langle E_s\cdot R\rangle_{scaled} = \Delta p = \{W^c/R\}^B \quad (10)$$

This relationship is used as a diagnostic parameter for earthquakes in Figure 2. Since this expression arises directly from the pressure wave amplitude relationship, Equation (1), divided by the leading constant factor K, it can also readily be called the normalized pressure wave amplitude factor. An example of the deduced behavior as a function of these parameters (seismic magnitude, scaled energy range, etc.) is shown in Figures 1 and 2.

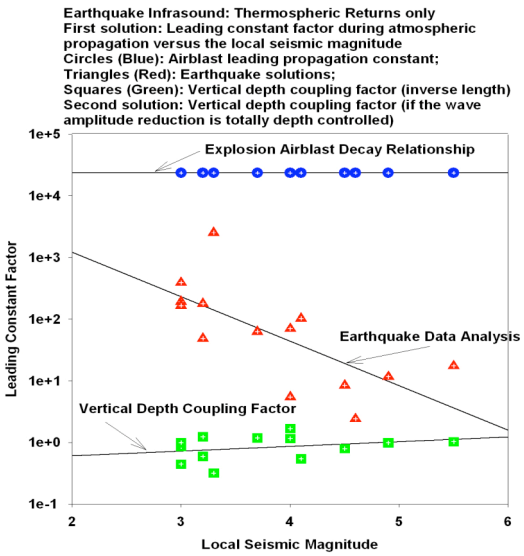

Figure 1. Leading constant propagation factor and the vertical depth coupling factor, k_{EQ} (in km^{-1}), versus the local seismic magnitude.

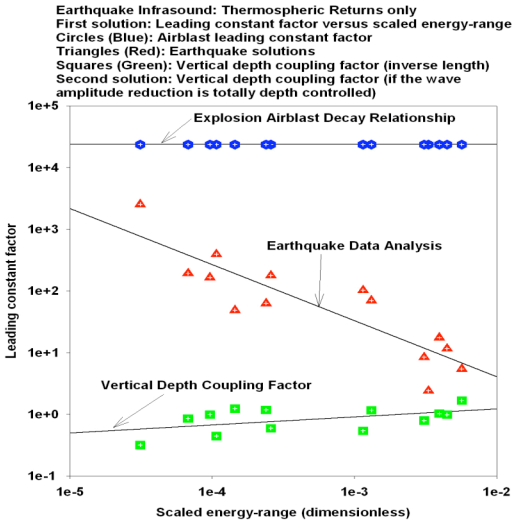

Figure 2. Leading constant propagation factor and the vertical depth coupling factor, k_{EQ} (in km^{-1}), versus the scaled energy-range.

From our analysis in Figure 1, it is evident that there is a single value of the leading constant propagation parameter for earthquakes that approaches the value of the atmospheric explosive blast wave solution propagation value, K. Presumably, this is also the local seismic magnitude where the depth of the recorded earthquakes also approaches zero (since this is observed to occur in Figure 1 at a local seismic magnitude of ~0). Similarly, the factor k_{EQ} is small for small earthquakes while its value steadily increases as the local seismic magnitude progressively increases. This is observed to be the inverse behavior of the leading constant propagation factor, whose value steadily decreases as the local seismic magnitude increases, presumably as the depth of the earthquakes also steadily increases. Equations (7) and (8) have been curve-fitted using a simple four-parameter Gaussian regression whose least squares correlation coefficient squared, $r^2 = 0.83132$ for the earthquake depth versus the vertical depth scale factor, D_{EQ}, as shown in Figure 3, whereas $r^2 = 0.6953$ was achieved for the vertical depth coupling coefficient, k_{EQ}, as shown in Figure 4 (with a single earthquake depth value at exactly $z = 0$ having first been removed from the data set to avoid division by zero and its implications).

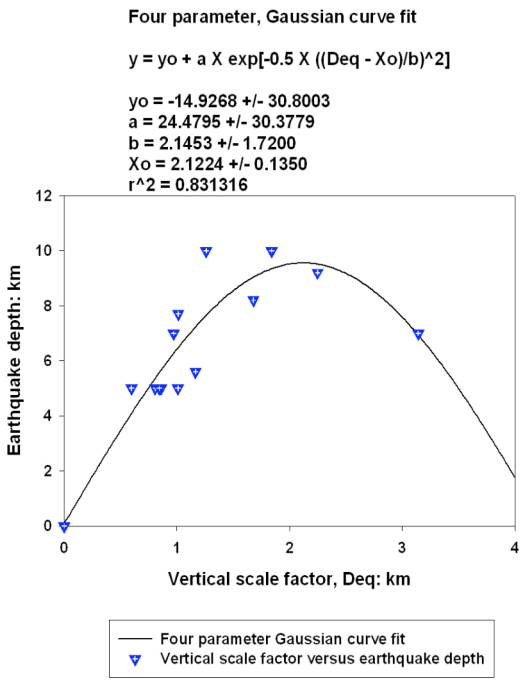

Figure 3. Earthquake depth versus the deduced vertical depth scale factor, D_{EQ} (km).

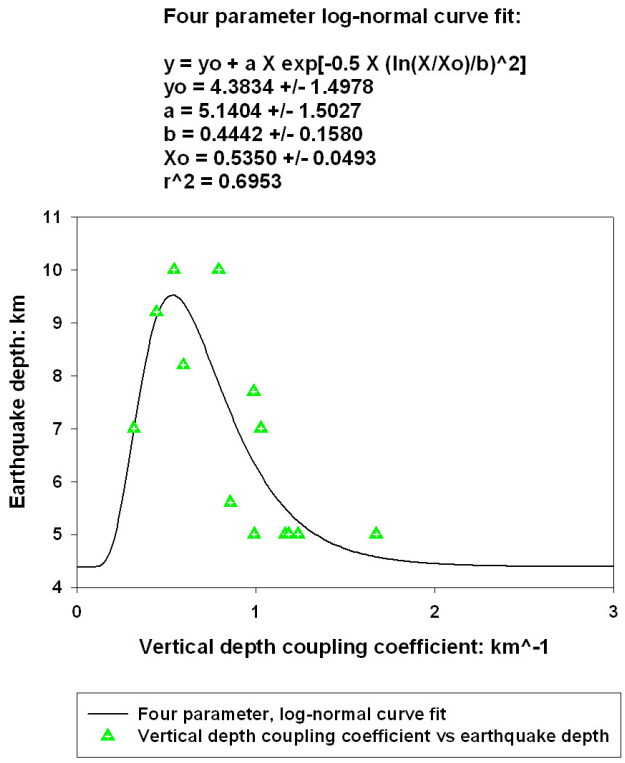

Figure 4. Earthquake depth versus the deduced vertical depth coupling coefficient, k_{EQ} (in km^{-1}).

The resulting curve-fit indicated in Equation (7) and shown in Figure 4 is only one of several regression curve-fits that we attempted, but all of our results indicated the same general form of curve-fitted behavior, with generally only small variations in (a, b, x_0), etc., and in the resulting maximum r^2 value.

Thus, the infrasonic amplitude (mean four-channel averaged value expressed in Pa) for Thermospheric returns can be now expressed in the following form:

$$\Delta p = K\cdot\{W^c/R\}^B\cdot\exp[-z/D_{EQ}] = K\cdot\{W^c/R\}^B\cdot\exp[-z/(x_0 \pm b\cdot\{-2\cdot\ln((z-y_o)/a)\}^{1/2})] \quad (11a)$$

We finally obtain the transcendental equation for the earthquake depth as a function of observed parameters:

$$z/(x_0 \pm b\cdot\{-2\cdot\ln((z-y_o)/a)\}^{1/2}) = -1.0\cdot\ln[(\Delta p/K)\cdot(W^c/R)^{-B}] \quad (11b)$$

or examining changes in z/D_{EQ}:

$$\delta(z/D_{EQ}) = z/(x_0 \pm b\cdot\{-2\cdot\ln((z-y_o)/a)\}^{1/2}) + \ln[(\Delta p/K)\cdot(W^c/R)^{-B}] \sim O(0) \quad (11c)$$

Equations (11b) and (11c) were formally solved by iterating very small values of D_{EQ}, while z, the earthquake depth, was evaluated using Equation (7). To accomplish this, we assumed that the difference between the two sides of the equation had to be less than a threshold value, which was assumed after trial and error to be ≤ 0.05 %.

From these curve fits, we have produced plots of the predicted earthquake depths (in km) as a function of range versus the local seismic magnitude for two assumed values of the wave amplitude in Figures 5 and 6 (for $\Delta p = 20$ and 2 Pa, respectively). Equivalently the same earthquake depth information is displayed in Figure 7 for $\Delta p = 20$ Pa, at various assumed horizontal ranges versus the source energy. These plots are presented directly below and were purposely computed for values slightly outside the original range of measurements that were documented in earlier reports.

In Figure 5 we have plotted our numerical solutions of Equations (11b) and (11c) for ***positive*** earthquake depths for the following extrapolated range of parameters with the observed earthquake parameters indicated in parentheses:

(1) $\Delta p = 0.02$ to 20.0 Pa (Observed amplitudes: 0.007 to 0.118 Pa)

(2) R = 320.0 to 5,000 km (Observed horizontal range: 206.9 to 1370.0 km)

(3) $W = 0.01$ to $1.0\cdot10^4$ kt (Observed source yield range: 0.0316 to 177.83 kt)

(4) M = 2.6667 to 6.6667 (Observed magnitude range: 3.0 to 5.5)

Numerical solutions of the earthquake depth as a function of the above parameters clearly show the following:

(1) Earthquake depths maximize at larger seismic magnitudes as either range increases or amplitude increases.

(2) The multi-valued nature of the solution is clearly evident in these plots since earthquake depths maximize as a function of the seismic magnitude and infrasonic amplitude at all selected ranges. This maximized behavior is produced by our simple Gaussian regressions expressed in curve-fit form in Equation (7).

It should be noted that the final values of the earthquake depths are slightly sensitive to all of these assignments but especially for the product c·B (see below for further discussion on this point). A complete sensitivity analysis of this system of equations will be performed shortly.

To illustrate the interpretation of the results, we will choose an example. If we have an infrasonic $\Delta p = 20.0$ Pa for R = 320 km and for $M_R < \sim 2.67$ (0.01 kt), all computed earthquake depths are very shallow, and the event could possibly be of man-made origin. Conversely, at the same range, if $M_R > \sim3.0$ (0.032 kt), but $M_R < \sim6.67$ ($1.0\cdot10^4$ kt), all computed depths are quite large, which effectively rules out a man-made source origin. However, for still larger observed seismic magnitudes, a significant decrease in the predicted depths again appears and the possibility of man-made sources again arises.

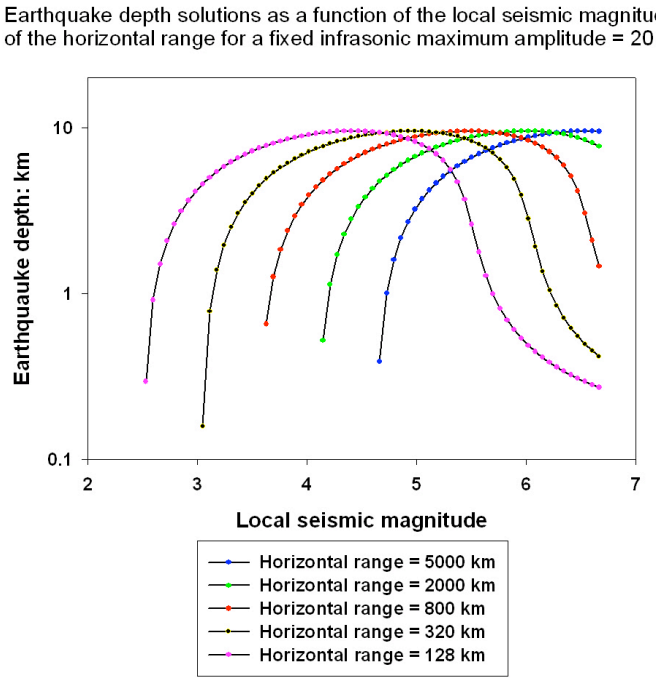

Figure 5. Earthquake depth (in km) versus the local seismic magnitude and the horizontal range for a fixed maximum infrasonic wave signal amplitude = 20 Pa.

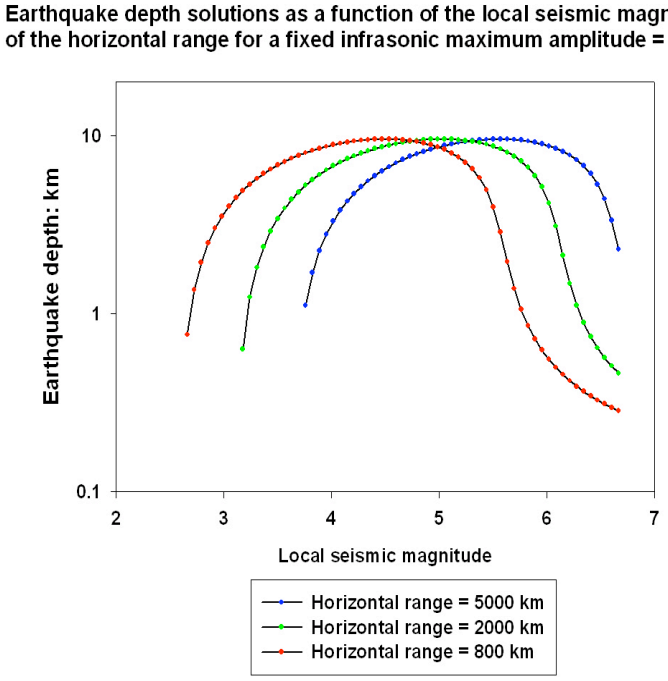

Figure 6. Earthquake depth (in km) versus the local seismic magnitude and the horizontal range for a fixed infrasonic maximum signal amplitude = 2.0 Pa.

Finally, we also have plotted these solutions as a function of the source energy in Figure 7.

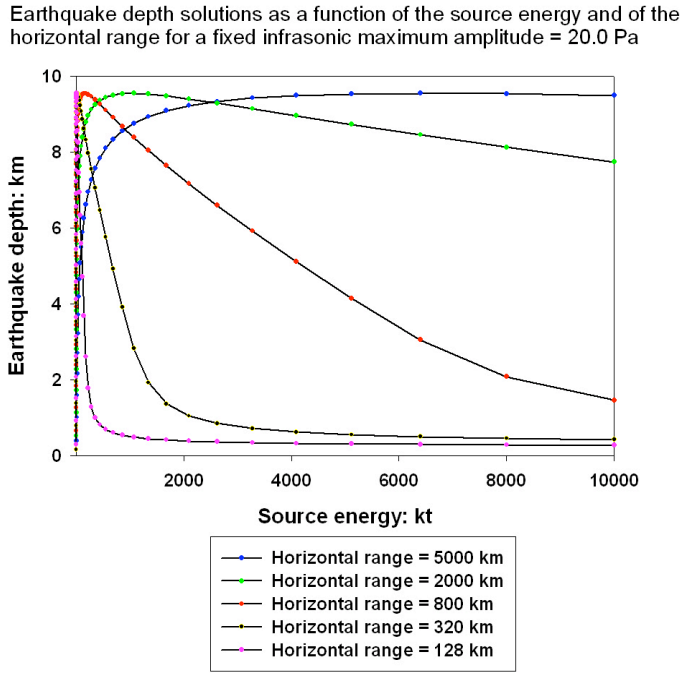

Figure 7. Earthquake depth (in km) versus the source yield (in kt) and the horizontal range for a fixed infrasonic maximum signal amplitude = 20.0 Pa.

For comparison, we present a bubble plot of the original 15 observed earthquake depths available from the USGS 2000–2002 database from our infrasonic detections at DLIAR. Depths are indicated within each bubble, while the relative bubble size is also indicative of the earthquake depth.

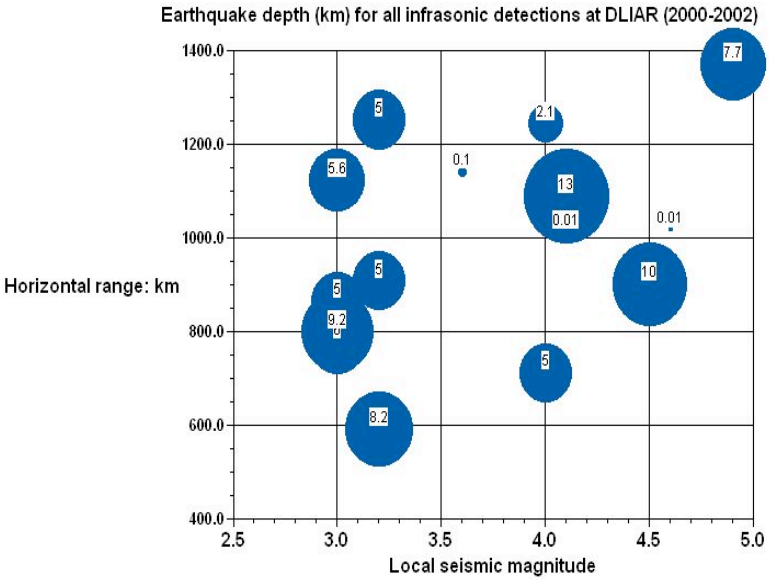

Figure 8. Observed earthquake depth (in km) versus the horizontal range and local seismic magnitude.

As a further example of the predicted behavior, consider a signal arriving from an unknown source that has been detected only infrasonically so that the source depth is fundamentally unknown except for the predictions for the set of equations developed in this paper. If the type of the signal is also unknown and if we assume that it is from an earthquake, we can still deduce the depth, knowing the horizontal range to the source, the maximum infrasonic wave amplitude, and the local seismic magnitude—or equivalently, a source energy estimate related to either a seismic magnitude, as shown earlier in Equations (9a) and (9b), or from the infrasonic wave period at maximum amplitude, etc. Assume the following observed parameters (for horizontal range, seismic magnitude, and wave amplitude):

Horizontal range = 1,500 km

Local seismic magnitude = 3.70 (W = 0.3548 kt)

Infrasonic amplitude = 10.0 Pa

From these parameters, we can deduce the vertical depth scaling factor, D_{EQ} = 4.160 km (k_{EQ} = 0.2404 km^{-1}) and the source depth = 0.662 km, if the source was an earthquake. It is very unlikely that a mining blast could be detonated at such a depth (662 m). As an alternative, consider the following set of recorded parameters:

Horizontal range = 100 k

Local seismic magnitude = 6.66 (W = 10^4 kt)

Infrasonic amplitude = 300.0 Pa

From these parameters, we can deduce the vertical depth scaling factor D_{EQ} = 0.1565 km (k_{EQ} = 6.39 km^{-1}) and the source depth = 1.159 km, if the source was an earthquake. It is extremely unlikely that a mining blast could be detonated at such a depth. If we further increase the amplitude to 3000 Pa (= 300 μbars) and keep all other factors held fixed, the source depth = 9.319 km, which certainly rules out a man-made underground explosion source. Further increases in amplitude, with all other parameters fixed, produce a decrease in the source depth, however. The reliability of the deduced infrasonic depth is only as good as the initial seismic calibration of the earthquakes analyzed earlier (for full details see ReVelle, 2005). If no seismic data are available for a set of infrasonic signals, we can still estimate the depth for the unknown signals by "crossing the beams" from multiple infrasonic arrays. This leads to the relative location as well as the horizontal range to the source, using the back azimuths of the analyzed signals. We can also measure other signal parameters and determine an independent source energy estimate, perhaps from the wave period at maximum amplitude of the signals or information that may be available from other external sources. Our final results are somewhat sensitive to the input parameters utilized but especially to the product, c·B, which has the possible ***far-field*** values $0.60 \leq c \cdot B \leq 0.725$, while we have used c·B = 0.68.

CONCLUSIONS AND RECOMMENDATIONS

On the basis of our results, we can say with confidence that given an infrasonic impulsive signal observation, we can reliably evaluate the value of the depth of the source if it was an earthquake. For sufficiently great depths, the event in question cannot be due to mining blasts, which are normally detonated quite close to the earth's surface.

REFERENCES

American National Standards Institute (1983). Estimating airblast characteristics for single point explosions in air, with a guide to evaluation of atmospheric propagation and effects, ANSI S2.20-1983 (New York: AIP).

Mutschlecner, J. P., and R. W. Whitaker (2005). Infrasound from earthquakes, *J. Geophys. Res*. 110: D01108, 1–11.

Reed, J. W. (1972a). Attenuation of blast waves by the atmosphere, *J. Geophys. Res*. 77: 1,616–1,622.

Reed, J. W. (1972b). Airblast overpressure decay at long range, *J. Geophys. Res*. 77: 1,623–1,629.

ReVelle, D. O. (2005). Additional infrasonic studies of earthquakes and mining blast discrimination, in *Proceedings of the 27th Seismic Research Review: Ground-Based Nuclear Explosion Monitoring Technologies*, LA-UR-05-6407, Vol. 2, pp. 845–854.

Sakurai, A. (1965). Blast wave theory, in *Basic Developments in Fluid Dynamics*, M. Holt (Ed.). New York: Academic Press), Vol. 1, pp. 309–375.